CHAPTER II:

SUPRAMOLECULAR ASSEMBLIES

II.1.0 INTRODUCTION

II.1.1 GENERAL

In the previous chapter, the structure-property relationship of macromolecules was discussed in terms of preparation methods. Equally important relationships can be derived based on polymeric architecture. [1a] More to the point, macromolecules of differing topology experience unique motional constraints as well as solvation effects, entanglements, etc., all of which greatly influence behavior. [2]

Polymeric architectures have historically been defined in a broad sense according to the number of chain ends present. This somewhat crude system of classification yields surprisingly consistent structure-property relationships. Figure 1 lists multiple polymeric architectures based on covalently bonded macromolecules. Classes I-IV are listed in the order of increasing number of chain ends.

Figure 1. Covalent Polymeric Architectures

Class I. Cyclic Polymers

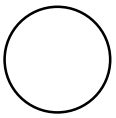

Class II. Linear Macromolecules
Homopolymers

$$—(A)_n—$$

Copolymers

$$—(A)_m\text{-}(B)_n—$$

Class III. Branched Polymers
Graft Copolymers

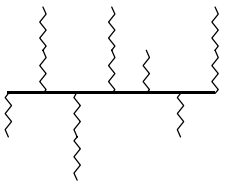

Star Polymers

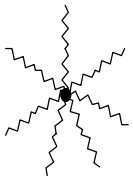

Class IV. Networked Polymers

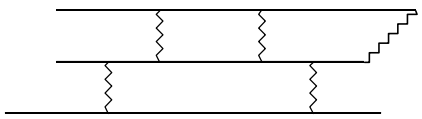

Hyperbranched/
Dendrimers

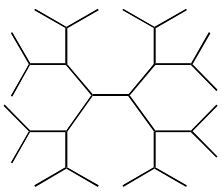

Class I represents cyclic polymers, which are void of chain ends altogether. Typically prepared by the aforementioned anionic route, [3] cyclic macromolecules show lower hydrodynamic volumes (and thus low intrinsic viscosities) as well as higher glass or melting transition temperatures than those of their linear counterparts. [4]

Their linear counterparts fall into the second class of polymers, which are broken into subcategories according to chemical makeup. While a homopolymer is comprised of one single repeat unit making up the polymeric backbone, a copolymer incorporates two or more unique repeat units into its chemical makeup. The number and type of repeat units, as well as its molecular weight distribution largely determine the properties of a linear homopolymer. [5a]

The properties of linear copolymers are equally dependent on the number, type, and distribution of monomeric makeup. [5] However, the order of monomer arrangement as well as overall composition plays a vital role in macromolecular properties. Defining an AB copolymer as a macromolecule consisting of a mixture of monomer A with monomer B, there are then three general arrangements of monomer possible. Whereas random copolymers exhibit statistical distributions of monomers A and B (Figure 2a), no single backbone A or B monomer is ever paired with itself in alternating copolymers (Figure 2b). Thirdly, block copolymers exist when like monomers react preferentially with themselves to yield long sequences along the backbone before reacting with a chemically dissimilar monomer, which again couples preferentially to itself (Figure 2c). Random and alternating copolymers tend to average the properties of the respective homopolymers in proportion to the relative abundance. In addition, alternating copolymers have regular order, which can greatly affect physical and chemical properties. [6] Phase separation in random and alternating copolymers is not an issue as long monomeric sequencing is limited.

Compare this to block copolymers, in which the chemically dissimilar sequences tend to phase separate due to non-mutual miscibility. Ergo, block copolymers often develop some of the properties of the individual blocks and can even form reversible

Figure 2. Random, Alternating, and Block Copolymer Sequencing.

a 

b 

c 

physical crosslinks through micro-phase domain separation that acts as a crosslinking anchor. [1b,7]

The third class of polymer topology involves branched polymers, which are broken into subcategories based on branch anchors. Star polymers have a central anchor from which a series of approximately equal length branches emanate. [5b] This results in a low radius of gyration and a subsequently low intrinsic viscosity. Dendrimers are regularly branched homopolymers comprised of a central core from which successive branches split to derive subsequent generations of larger macromolecules. Physical interest in these tree-like molecules stems from their controllable size, preorientation, solubilization and polarity. [8] Finally, graft copolymers are defined by the attachment of chemically distinct macromolecules onto a central backbone. A subset of graft copolymers, comb polymers graft chemically distinct macromolecules of equal chain length onto a central backbone in a uniform and regular fashion. Much like block copolymers, the physical behavior of graft copolymers varies according to chemical composition and can be tailored to introduce specific traits. [9]

The fourth topological class involves networked, or crosslinked, polymers in which a three dimensional network is formed via intertwined, covalently bonded macromolecular chains. Chain rigidity and transition temperatures increase with

crosslinking due to a reduction of free volume, or configurational entropy, although it should be noted that highly crosslinked polymers may not show an observable transition at all. [5c] As a result, crosslinked materials show dimensional, solvent, and heat stability. [10a]

Figure 3 introduces topological concerns addressing non-covalently bonded networks. Not shown is the case of polymer blends, in which two or more polymers are mechanically mixed together. Depending on the miscibility of the blended macromolecules, unique properties often arise that do not otherwise exist. If the polymers blend at the molecular level, an averaging out of the individual component properties is commonly found. [11] If phase separation occurs, we observe behavior similar to that found in block copolymers. Interestingly, the mechanical shearing involved in mixing the polymer blend may result in homolytic cleavage of bonds, followed by recombination to form secondary block or graft copolymers which may again exhibit different properties from those of the non-sheared polymer blend. [10b]

Figure 3. Non-covalent Polymer Topologies.

Interpenetrating Polymer Networks (IPNs):

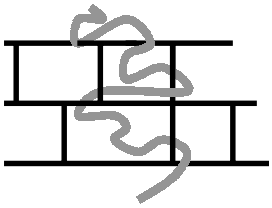

Rotaxane or Pseudorotaxane Based Macromolecules

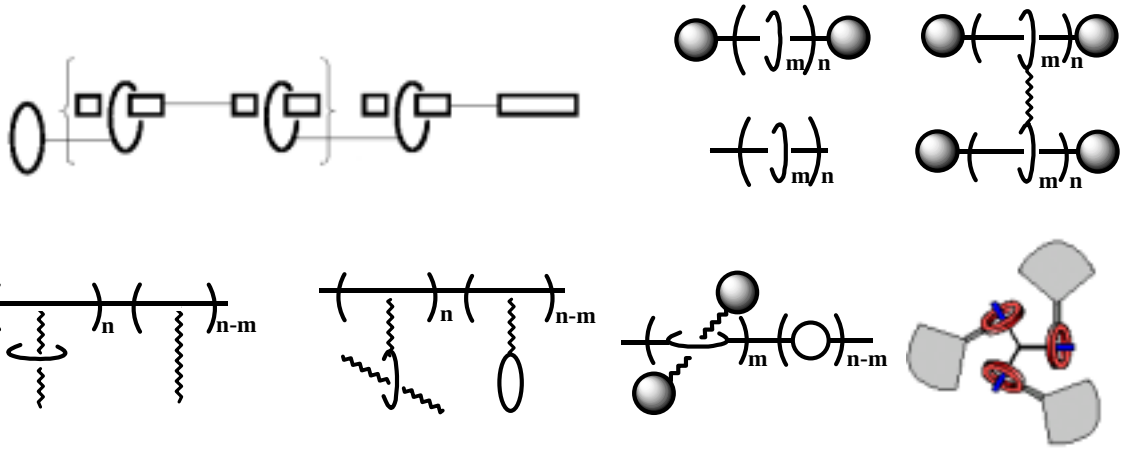

Interpenetrating networks, or IPNs, involve a non-covalent interaction between two or more individually crosslinked polymers. These networks are prepared by polymerizing and crosslinking one polymer in the presence of a pre-fabricated networked polymer, resulting in a permanent mixture often referred to as a supramolecular blend in which two or more molecules are related by non-covalent forces. IPNs behave as normal networked systems (insoluble, dimensional stability, etc.), in addition to experiencing an averaging out of the individual component properties. In this regard, catenanes and rotaxanes may be thought of as subsets of interpenetrating networks.

II.1.2 SELF ASSEMBLED SUPRAMOLECULAR TOPOLOGIES: ROTAXANES, PSEUDO-ROTAXANES, CRADLED BARBELLS, POLY-ROTAXANES, AND POLYPSEUDOROTAXANES

In 1961 Frisch and Wasserman extended the idea of non-covalent topologies to the area of pseudorotaxanes **1**. [12] Although no experimental evidence could be found at the time for the existence of such a novel architecture, the particular area of interlocking ring systems had intrigued multiple scientists. [13] Frisch and Wasserman described **2** as a cyclic molecule threaded by a linear species with bulky groups at both ends that inhibit dethreading of the macrocycle. The subsequent complex was coined a rotaxane, derived from the Latin words for wheel and axle. [14] This can be contrasted to a pseudorotaxane **1** in which the threaded unit is void of bulky end groups, and a catenane **3**, comprised of interlocking rings. Although the preparation of rotaxanes and catenanes are closely related to each other, [15] this chapter will focus specifically on rotaxane and pseudorotaxane motifs.

Figure 4. Pseudorotaxane **1**, Rotaxane **2**, and Catenane **3** Cartoons.

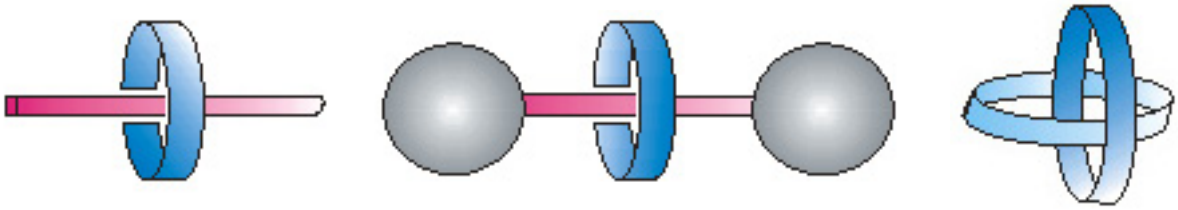

1 **2** **3**

II.1.2.1 ROTAXANES, PSEUDOROTAXANES, AND CRADLED BARBELLS

1967 saw the first experimental evidence of rotaxane formation by two independent research groups. While Schill and Zöllenkopf examined rotaxane formation by a multi-step and tedious chemical conversion method, [14] Harrison and Harrison utilized the laws of statistics to prepare rotaxanes using a polymeric support. [16] Here, the hemisuccinate ester of 2-hydroxycyclooctancosane was bound to a Merrifield resin and allowed to interact with 1,10-decanediol prior to addition of trityl chloride. The resin was then washed and the process repeated 70 times before the products were liberated from the resin by hydrolysis, giving a rotaxane in 6% yield.

Harrison later went on to modify this statistical approach by showing the formation of rotaxanes via 1) "slippage," a kinetic process and 2) reversible capping equilibria, a thermodynamic process (Scheme 1). [17] In both cases, an unspecified mixture of cyclic hydrocarbons was introduced to 1,10-bis(triphenylmethoxy)decane at 120 ^{o}C. In the reversible case, a catalytic amount of trichloroacetic acid was added to enable reversible detachment of the bulky triphenylmethoxy end groups.

Scheme 1. A) "Slippage" and B) Reversible Capping Approaches to Rotaxane Formation.

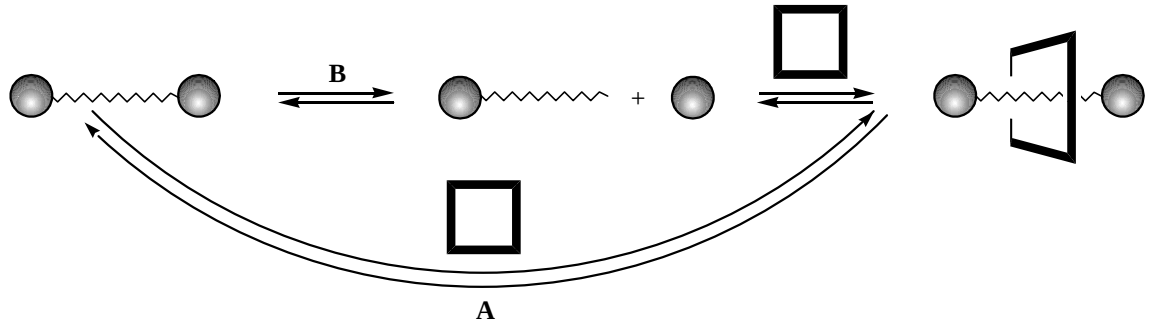

Harrison was able to show that in the thermal route, a rotaxane **2** that contained only the 29 membered cyclic chain was formed. He reasoned that the thermal energy enabled large rings, in this case rings greater than 28 methylene units, to "slip" over the bulky end groups and afford the rotaxane **2**. Additionally, rings larger than 30 units were not retained by the blocking groups once threaded.

In the reversible route, Harrison determined that threading of macrocycles smaller than 29 units could occur. Importantly, he showed that for a macrocycle to thread a straight chain alkane void of bulky end groups, the ring must be at least 23 units large. Further work in this area established blocking group effectiveness and the influence of linear chain length on the formation of rotaxane complexes. [18,19]

A major impetus for the investigation of rotaxane formation derived from the discovery that dibenzo-18-crown-6 (**4**) [20] formed a complex with alkali ions in a selective manner (see Scheme 2). [21a,b] This finding was especially important since the alkali and alkaline earth metals are involved in many physiological processes, thereby imparting potentially useful pharmaceutical applications to the crown ether. [22]

Due in large part to the identification of these macrocycles as simple enzyme mimics, crown ethers have shaped the area of host-guest chemistry almost simultaneously with the emergence of rotaxane architectures. First defined by Cram, [23] host-guest chemistry has been broadly defined as a supramolecular event in which two molecules

Scheme 2. Binding of Alkali Ions by Dibenzo-18-crown-6 (**4**).

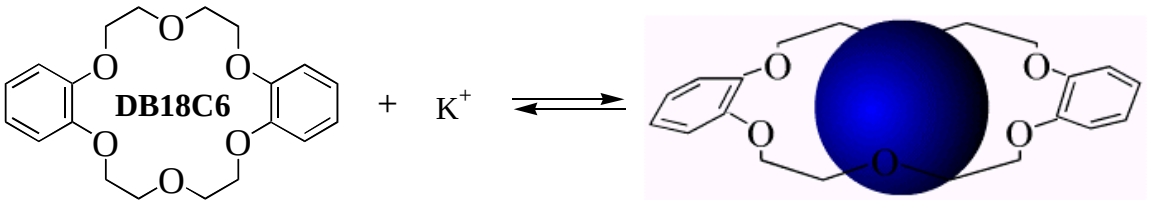

4

simultaneously recognize each other and form a complex of some sort, where the larger molecule is referred to as the host. In the case of Pederson's ionophores, the electron deficient cation could be lipophilized by the crown ether through interaction with the non-bonding oxygen electrons. Here, the crown ether acts as a host to the cation guest.

The ability of crown ethers to complex other ligands such as ammonium and alkylammonium salts was later shown by Pedersen and Frensdorff. [24,25] In 1975, Goldberg demonstrated the formation of a complex between *t*-butylamine (**5**) and the acidic form of 3,6,9,12,15-pentaoxa-21-carboxybicyclo[15,3,1]heneicosa-1(21),17,19-triene, commonly referred to as 2-carboxy-1,3-phenylene-18-crown-6 (**6**) (Figure 5). [26] Though not a pseudorotaxane in the sense that the ammonium ion does not extend through the cavity of the crown ether[†], the interaction between host and guest in complex formation had begun to make a strong case for template directed synthesis of rotaxanes and pseudorotaxanes. Notably, half a decade after Harrison's pioneering statistical threading efforts, Zilkha and coworkers published two papers describing the formation of rotaxanes and catenanes from benzo-crown ethers and oligo(ethylene glycol)s (see Scheme 3). [27,28]

Figure 5. Complexation of *t*-Butylamine (**5**) by 2-carboxy-1,3-phenylene-18-Crown-6 (**6**).

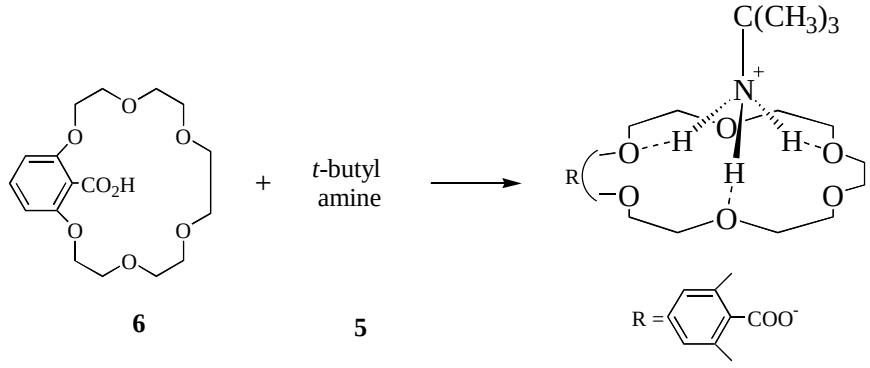

[†] Such a formation is often referred to as a perching complex.

Although results say otherwise, Zilkha et al. thought their pseudorotaxanes to be formed by statistical threading. In fact, the threading yields were much higher than the laws of statistics would suggest: they found up to 63% of added macrocycle threaded upon adding equimolar amounts of diols and crowns! Their results also indicated that pseudorotaxane formation was increased until the ratio of macrocycle to linear diol reached two and then remained constant. It was shown that the degree of threading increased with crown ether cavity size, while threading was independent of linear chain length. All of these factors lead the discerning eye to one conclusion: dipole-dipole attractions, here in the form of hydrogen bonding between the basic hydrogens of the alcohol and the electron rich oxygen atoms of the macrocycle (Scheme 3), can be applied and utilized as a major driving force for rotaxane formation.

Subsequent investigations into this newly defined template directed approach to rotaxane formation, in which host-guest interaction readily occurs, support Zilkha's experimental work. Cram and others manipulated the N-H···O interaction to discover that 27-crown-9 complexes guanidinium with 1:1 stoichiometry. [29] Metcalf et al. published a manuscript detailing the complexation of *N*,*N*-dimethyldiaza-12-crown-4 with various secondary ammonium ions. [30] Similarly, Stoddart and co-workers bound ammonia to a transition metal cation, thereby acidifying the N-H bonds and allowing the transition metal complex to be readily associated to a crown ether, in this case, 18-crown-6. [31] More recently, Gibson has synthesized polyamide, [32] polyurethane, [33] and polyester [34] rotaxanes utilizing aliphatic crown ethers as the host moiety. The results were predictably similar to Zilkha's experimental data, establishing beyond doubt the importance of H-bonding (Scheme 3) in the formation of diol- and amine-based rotaxanes and polyrotaxanes.

Scheme 3. Template Directed Pseudorotaxane Formation with Oligo(ethylene glycol)s and Benzo Crown Ethers (see text).

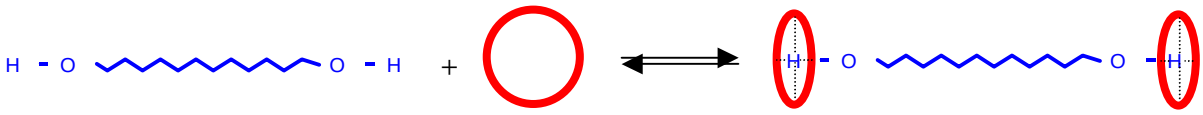

These clever experiments take advantage of unique interactions between host and guest molecules, which ensure complex formation. In this manner, the field of "self-assembly" was birthed. Whereas the earlier supermolecules were produced utilizing traditional reaction sequences, these new assemblies were constructed simply by building into each component the attribute of recognition. Hence, a mixture of the host and guest component spontaneously leads to an energetically favored complex: they are self-assembled.

A natural and logical progression in the area of host-guest interactions, further work focused on the enhancement of the self-assembly process. Early efforts involving 18-crown-6 showed that the structures of uncomplexed and complexed 18-crown-6 vary dramatically. [35] In the free state, two methylene groups occupy what would otherwise be a void in 18-crown-6. The fact that these two groups rotate outwards in the presence of K^+ to create the cavity in which the metal cation will reside (thereby exhibiting D_{3d} symmetry) is an excellent example of how nature loathes a vacuum (Figure 6). Given specific initial conditions, the most energetically favored conformation will be adapted by the floppy macrocyclic hosts.

Figure 6. Various Conformation of 18-crown-6.

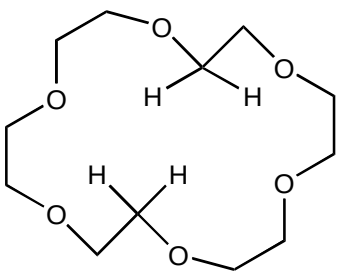

18C6 in
Free State

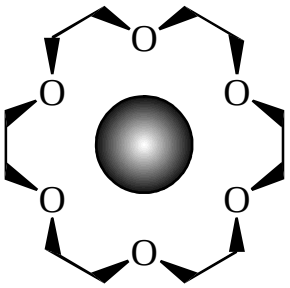

Complexed
18C6

While the barrier to inversion may be sufficiently small to allow complexation to occur within the simple crown ether macrocycles, it necessarily follows that such a host is not optimized for inclusion of guest species. This becomes readily apparent upon studying Table 1 and Figure 7. [36] The [2.2.2]-cryptand (so named for the two donor atoms each incorporated within the three armed, bridged macrocycle) can be thought of as an inflexible simple crown ether where inversion has been eliminated due to the rigidity of the compound. Valinomycin, on the other hand, is a 36-membered natural antibiotic transport ring that is capable of adopting multiple conformations.

Assessment of potassium cation binding constants, K_a, suggests that association is strongest in the inflexible cryptand, just as one may expect due to entropic reasoning: the inherent loss in entropy associated with rearrangement might be thought to ultimately have the effect of reducing overall free energy, thus giving a negative push on equilibrium towards uncomplexed constituents. Interestingly, association by the relatively large and conformationaly flexible valinomycin dwarfs that by the smaller 18-crown-6. Further investigation of potassium release rates provides consistent insight. Again just as one might expect, release rates vary according to strength of binding: 18-crown-6 more readily gives up the potassium cation than does the [2.2.2]-cryptand. Keeping in mind that valinomycin is a flexible molecule, it becomes obvious that a host molecule that can bind the cation in a three-dimensional array of donor groups will demonstrate strong binding ability while protecting the guest from the lipid environment. On the flip side, a host that is permanently set in the three-dimensional array does not readily give up the complexed guest. The guest is trapped within a cage, so to speak, whereas compounds that can encapsulate guest moieties by conformational rearrangements have the unique ability to open up their cavities to allow cation transport. As an example: valinomycin adopts a three-dimensional “tennis ball seam arrangement” about the cation by utilizing intramolecular hydrogen bonding and can open up these seams in the proper environment. [37] At the other extreme, simple crown ethers are not large enough to fully encapsulate most guest molecules, thereby ensuring a weaker binding constant than the three-dimensional array permits. Consequently, the smaller crown allows multiple points of attack on the bound cation, ensuring a facile releasing mechanism. There are advantages and disadvantages of each.

Table 1. Potassium Cation Binding Strengths and Rates for Various Ligands in Water at 25 ^{o}C. [36]

Ligand	K_a (M^{-1})	k_1 [a] ($M^{-1}s^{-1}$)	k_{-1} [b] (s^{-1})
18-crown-6	115	4.3×10^8	7.5×10^6
[2.2.2]-cryptand	200,000	7.5×10^6	380
valinomycin[c]	31,000	4.0×10^7	1.3×10^3

[a] binding rate constant

[b] decomplexation rate constant

[c] values determined in anhydrous methanol

Figure 7. Molecular Structures of 18-Crown-6, Valinomycin, and [2.2.2]-Cryptand.

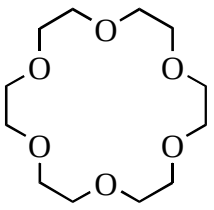

18-crown-6

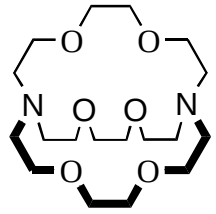

[2.2.2]-cryptand

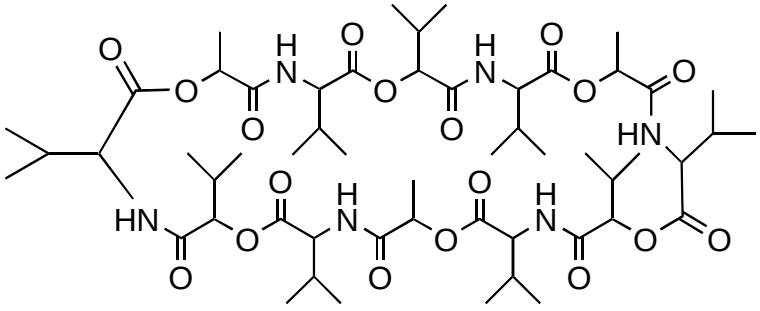

valinomycin

Furthering this discussion before returning to a more general introduction, it has recently been shown that simple crown ethers have the ability to adopt at least two distinct structures upon complexation: the simple inclusion species such as rotaxanes and metal bound substrates *in addition to* "cradled barbell," or hot-dog like structures with larger guest molecules in which the host wraps around the guest moiety (see Figure 8). [38] The suprastuctures formed are so called "exo" complexes. Host flexibility, intramolecular substituent interactions, and neighboring molecules through-space communication all appear to influence the nature of complex formation. [38] Due to these recent investigations, care has been taken in Section II.2 to avoid assuming all host:guest networks investigated form *only* pseudorotaxane complexes. In fact, "cradled barbell" and pseudorotaxane structures may co-exist simultaneously. Furthermore, and although solid state structures have been solved for a great number of crown ether:guest salts, there is continuing controversy as to the behavior of these structures in solution and the gas phase.

Figure 8. Space Filling Diagram Illustrating the Cradled Barbell Structure. [38b]

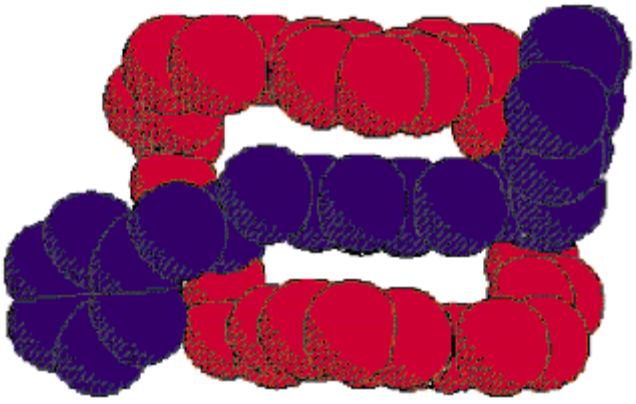

To understand the mechanism of host-guest interactions, and as hinted at above, researchers looked at binding constants as well as the thermodynamic parameters of entropy (ΔS) and enthalpy (ΔH) and then tried to compare the values among various systems--a daunting task given the difficulty in experimentally measuring the thermodynamic parameters. In addition, the experimental conditions imposed by researchers of the day such as varying solvent systems, using different guest counter ions, etc. rendered many comparisons meaningless. Nonetheless, there did exist systems worthy of comparison.

The pioneering work of Pedersen and Frensdorff [24,25] laid ground for observations of guest substituent effects. In particular, the effect of R on the binding constants for complexes of 18-crown-6 and R-NH_3^+ was shown be dramatic. In methanol, the binding constants (log K_a) of 18-crown-6 with $MeNH_3^+$, $EtNH_3^+$, $PhNH_3^+$, and *t*-$BuNH_3^+$ were shown to be 4.25, 3.99, 3.80, and 2.90, respectively. [39,40] Three N-H···O hydrogen bonds stabilize the system; the binding constants decrease as a function of steric influences. In addition to varying guest substituents, Gokel and others looked at the effect of varying donor atoms around the 18-membered crown ether hosts upon complexation with *t*-butyl ammonium thiocyanate (see Figure 9). [41] It had been shown as early as 1979 that azacrown ethers, crown ethers containing at least one nitrogen donor atom within the crown, form stronger complexes with primary ammonium ions than do the corresponding simple crown ethers. [42, 43] Varying the crown ether ring size also had dramatic effects on complexation with cationic guests (see Figure 9). Several researchers demonstrated that complexation of ammonium ions was favored by 18-membered rings over 12-, 15-, and 24-membered rings. [44]

In 1987, Stoddart and coworkers studied the complexation of paraquat dications with two larger crown ethers, bis *para*-phenylene-34-crown-10 (BPP34C10) and bis *meta*-phenylene-32-crown-10 (BMP32C10), to form pseudorotaxanes. [45] Nearly a decade later, Busch et al. and Stoddart and coworkers demonstrated the synthesis of a rotaxane from a crown ether and secondary ammonium ion. [46] Stoddart et al. then went on to report on a 2:1 guest:host pseudorotaxane formed by BPP34C10 with dibenzylammonium ions. [47]

Figure 9. Influence on Association Constants by Donor Atoms Around 18-Membered Crown Ether Hosts Upon Complexation with *t*-butyl Ammonium Thiocyanate in MeOH.

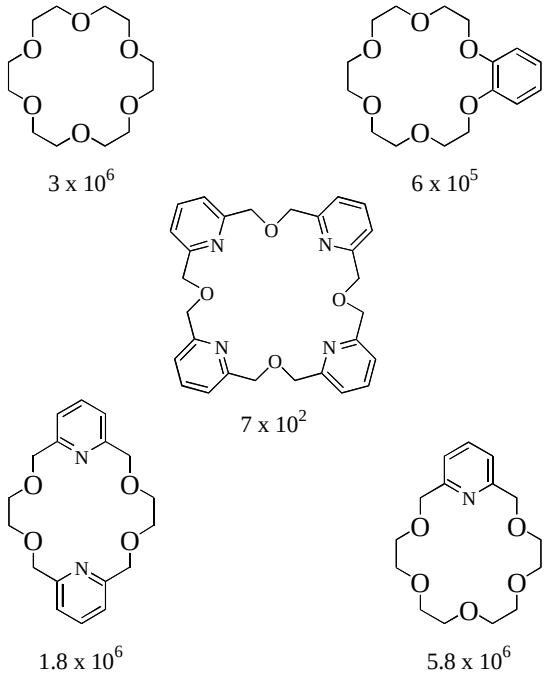

Working in parallel, Wang and coworkers investigated self-assembled solid state networks formed from secondary hydrogen bonding interactions. In 1990, they resolved the crystal structure of the two dimensional network formed between cyanuric acid and melamine (Figure 10). [48] This naturally occurring triply bonded recognition motif would go on to be a very useful building block of many directed approaches to induce supramolecular binding. [49] Such base pairing was not happenstance: natural arrays with three hydrogen bonds were forced into the limelight after Crick and Watson established the helical structure of DNA resultant from the base pairing between purines and pyrimidines. [50]

Recognizing the potential to add base pairs to pseudorotaxane guest moieties to promote interactions, Stoddart moved beyond the simple pseudorotaxane to establish larger aggregates approaching supramolecular polymers that could be controlled

Figure 10. Two Dimensional Network Formed Between Cyanuric Acid and Melamine. [48]

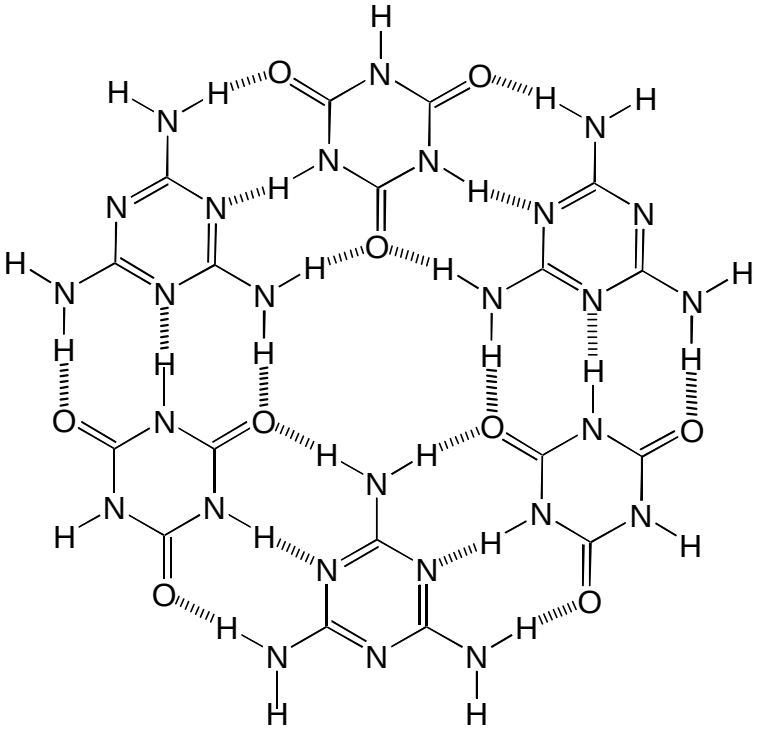

thermodynamically and were thus reversible. To do this, terminal carboxylic acid groups were added to a symmetrical secondary ammonium ion and allowed to associate such that intramolecular hydrogen bonding between acid functionalities occurred in a linear array. [51] Much of the current interest in supramolecular polymers involves quadruple hydrogen bond arrays, which have been predicted to be much more robust than triple and double hydrogen bond networks. [52] Recently, a small number of supramolecular aggregates have made use of the modest strength of association (which is comparable to many triply hydrogen-bonded systems) found in pseudorotaxane networks. [53] In particular, Gibson et al. have prepared a series of dendritic pseudorotaxanes using such self-assembling complimentary building blocks as a triply charged ammonium ion and various generations of benzyl ether dendrons bearing the dibenzo-24-crown-8 moiety. They have also prepared linear supramolecular pseudorotaxane polymers (see Figure 3).

II.1.2.2 ROTAXANES, PSEUDOROTAXANES, AND CRADLED BARBELLS: EXPERIMENTAL INVESTIGATIONS

The next two chapters will deal with first understanding the nature of association involved in complex formation of simple crown ether macrocycles with various guest moieties before moving on to enhanced or inhibited host-guest interaction based on more complex supramolecular assemblies involving immediate neighbor constituents. The reader is encouraged to read appendix I, which concerns the derivation of binding constants in some detail before continuing.

II.2.0 HOST/GUEST INTERACTIONS

As described in the introductory section 1.2, a pseudorotaxane consists of a linear guest unit that is threaded through the cavity of a macrocyclic host. Compare this to the "cradled barbell" in which the folded host macrocycle envelopes the guest ion, thereby exhibiting an "exo" complex. Although strong interactions may exist between host and guest such as π-stacking, dipolar-dipolar interactions, and H-bonding motifs, pseudorotaxane and "cradled barbell" formations are reversible processes. Determination of association constants and thermodynamic parameters allows one to quantify the strength of such supramolecular interactions.

Given equilibrium conditions as described in Equation 1, the macroscopic dissociation constant can be determined according to Equation 2.

$$nG + H \rightleftharpoons HG_n \qquad (1)$$

$$K_a = \frac{[HG_n]}{[H][G]^n} \qquad (2)$$

Tsukube and coworkers discuss in detail various techniques used to determine association constants. [54] Of particular interest to our lab, the use of proton NMR shifts at various host to guest ratios to determine K_a is described for systems when n = 1. There are two extreme exchange regimes commonly encountered in supramolecular assemblies: slow-exchange and fast exchange.

In the slow-exchange regime, two chemically dissimilar environments exist at a single moment in the NMR instrument's time scale: we see *both* the threaded pseudorotaxane **HG** as well as the unbound ligands **H** and **G** (Figure 11a). Utilizing the integration values of complexed (δ_{HG}) versus uncomplexed (δ_G) components affords a facile means to determine the percentage of complexed guest (or host) species, and knowing the precise concentrations of host and guest moieties added, one can readily

determine both the stoichiometry and association constants from one unique NMR experiment.

In the fast-exchange regime, a single, time-averaged peak is observed (Figure 11b). Thus, it is no longer possible to determine K_a based on the single point method. Instead, one must consider how the time averaging of the observed signal is derived and then go on to develop new multi-point methods based on this information; the Benesi-Hildebrand, Scatchard, Creswell-Allred, and Rose-Drago multi-point methods are described below.[†]

Figure 11. Two Commonly Encountered Exchange Rate Regimes in Supramolecular Assembly Formation: a) Slow Exchange, b) Fast Exchange.

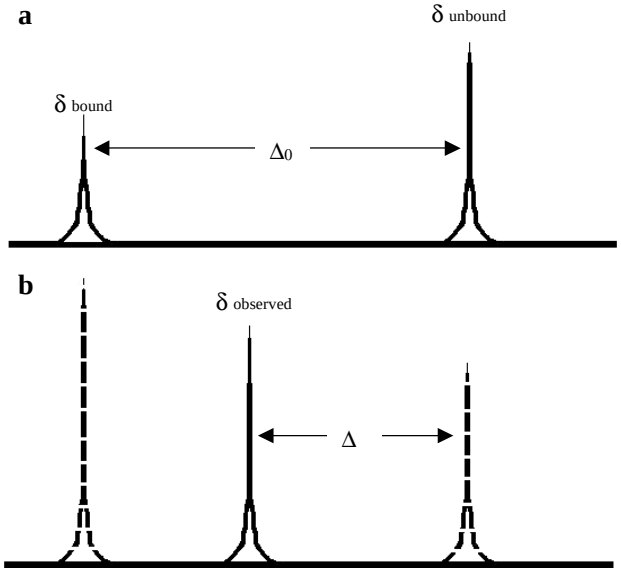

[†] See Appendix I for a more thorough discussion of the various methods used to determine association constants in supramolecular complexes.

II.2.0.1 BINDING MODELS: BENESI-HILDEBRAND METHOD

δ_G, or the chemical shift of an uncomplexed guest proton, and $\delta_{observed}$ are known from experimentation in fast-exchange systems. Not known are δ_{HG}, or the chemical shift of the fully complexed guest, and the mole fractions of complexed versus uncomplexed species N_{HG} and N_G. Equation 3 equates the observed time-averaged signal as a function of these parameters.

$$\delta_{obs} = N_{HG}\delta_{HG} + N_G\delta_G \tag{3}$$

and N_{HG} and N_G are defined as

$$N_{HG} = \frac{[HG]}{[G]+[HG]} \tag{4}$$

$$N_G = \frac{[G]}{[G]+[HG]} \tag{5}$$

Accordingly, the sum of N_{HG} and N_G must be unity.

$$1 = N_{HG} + N_G \tag{6}$$

Solving Equation 6 for N_G and substituting the answer and Equation 4 into Equation 3 gives

$$\delta_{obs} = \delta_G + \frac{[HG]}{[G]+[HG]}(\delta_{HG} - \delta_G) \tag{7}$$

Additionally, and according to Equation 1, the initial concentration of guest moieties $[G]_0$ can only go to unbound or bound species:

$$[G]_0 = [G] + [HG] \tag{8}$$

Equation 7 then becomes

$$\delta_{obs} = \delta_G + \frac{[HG]}{[G]_0}(\delta_{HG} - \delta_G) \tag{9}$$

Solving for [HG]:

$$[HG] = \frac{[G]_0(\delta_{observed} - \delta_G)}{(\delta_{HG} - \delta_G)} \tag{10}$$

As shown in Figure 11, Δ and Δ_0 are defined as

$$\Delta = \delta_{observed} - \delta_G \tag{11}$$

$$\Delta_0 = \delta_{HG} - \delta_G \tag{12}$$

Incidentally, the ratio Δ/Δ_0 is referred to as the saturation factor and is equivalent to $N_{HG,}$ or the fraction of bound guests θ. Thus

$$[G] = [G]_0 - \left(\frac{\Delta}{\Delta_0}\right)[H]_0 \tag{13}$$

Equation 10 can be rewritten

$$[HG] = [G]_0\left(\frac{\Delta}{\Delta_0}\right) \tag{14}$$

Solving Equation 2 for [G] and substituting into Equation 8 gives

$$[G]_0 = [HG]\left(\frac{1}{K_a[H]} + 1\right) \tag{15}$$

We then arrive at a derivation of the Benesi-Hildebrand [55] equation as discussed in Appendix 1 by substituting for $[G]_0$ in Equation 14 and rearranging the result

$$\frac{1}{\Delta} = \frac{1}{\Delta_0 K_a[H]} + \frac{1}{\Delta_0} \tag{16}$$

In fast exchange regimes, only Δ is known; Δ_0 and [H] and both unknown.

It should be noted that [H] and [G] may be used interchangeably in all the above equations. The specific equations utilized depend on which component is used to titrate the other: if specified concentrations of host molecules are continually added to a solution of guest moieties, Equation 16 should be used. In the case of pseudorotaxane and "cradled barbell" formation, the macrocycle is a neutral species whereas the guest is typically a salt. Titrating the salt with the host macrocycle avoids the danger of continually increasing the ionic potential of the solution. Often times, however, it is simply too costly to persistently add expensive and scarce macrocycles: it is much more economical to continually add guest salts to a set concentration of host macrocycle. [56]

Returning to our discussion on the usefulness of Equation 16, [H] has traditionally been approximated by $[H]_0$ in systems exhibiting low association constants. [54] Ergo, inverse values of Δ are plotted versus inverse values of [H] to yield a linear plot whose slope and intercept yield estimated Δ_0 and K_a values, respectively. Gibson et al. have improved this approximation by using an iterative technique in which they first allow $[G]_0$ (recall the interchangeability of [G] and [H]) to approximates [G], solve Equation 16 and then go on to use the calculated Δ_0 to refine the initial estimate of [G] by utilizing Equation 13. [57] This iterative process is repeated until continued iterations result in a constant Δ_0 and K_a.

II.2.0.2 BINDING MODELS: SCATCHARD METHOD

In an analogous fashion to that described in Appendix I, the Scatchard [58] equation may be derived using chemical shift changes as above.

$$\frac{\Delta}{[H]} = -K_a\Delta + K_a\Delta_0 \qquad (17)$$

Here, Δ / [H] is plotted versus Δ to yield a linear fit whose slope is equal to $-K_a$ and whose intercept is equal to $K_a\Delta_0$. Again, [H] may be approximated by $[H]_0$ and the iterative techniques described by Gibson et al. [57] applied to arrive at a more realistic value of [H].

II.2.0.3 BINDING MODELS: ROSE-DRAGO METHOD

In cases where it is inappropriate to assume that $[H]_0$ approximates [H], the Rose-Drago [59] method has been applied. [60] Here, $[H]_0$ is used and Δ_0 is assumed. According to Equation 18, graphs of various assumed Δ_0 values versus K_a^{-1} are plotted; the mean crossing values of each approximated fit are then used to estimate K_a.

$$(\Delta_0 - \Delta)K_a = \frac{\Delta\Delta_0}{\Delta_0[G]_0 - \Delta[H]_0} \qquad (18)$$

II.2.0.4 BINDING MODELS: CRESSWELL-ALLRED METHOD

The Cresswell-Allred [61] treatment has also been applied in cases where $[H]_0$ cannot be assumed to approximate [H]. [62] Observed δ values are plotted against $[HG] / [H]_0$ in the form of

$$\delta_{observed} = \frac{[HG]}{[H]_0}\Delta_0 + \delta_H \tag{19}$$

[HG] may be calculated by assuming an initial K_a according to the quadratic solution of the equilibrium constant expression, Equation 20; all other values are known. K_a is then adjusted until the intercept, δ_H, agrees with the known experimental value. [57]

$$[HG] = \frac{\left(\left([R]_0 + [S]_0 + \frac{1}{K_a}\right) \pm \sqrt{\left([R]_0 + [S]_0 + \frac{1}{K_a}\right)^2 - 4[R]_0[S]_0}\right)}{2} \tag{20}$$

II.2.1 FOUR SUPRAMOLECULAR COMPLEX INVESTIGATIONS

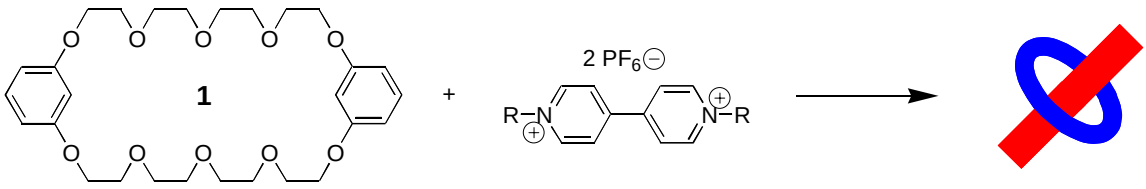

The complexation of bis(*m*-phenylene)-32-crown-10 (**1**) with N,N'-dialkyl-4,4'-bipyridinium salts, i.e. paraquats or viologens, has been well known since 1987, when Stoddart et al. determined the association of dimethyl paraquat with **1** to be on the order of 760 M^{-1} in acetone. [45] Gong and others [63] have gone on to study the complexation of substituted BMP32C10 macrocycles with various paraquat ions. The following sections reanalyze and compare four such pseudorotaxane and/or "cradled barbell" systems. In every case, previously collected ^{1}H NMR data has been used for reanalysis.

II.2.1.1 EXPERIMENTAL

Macrocycles **2**, **4**, and **6** were prepared by Gong using reported procedures. [63, 64] Guest paraquat ions **3**, **5**, and **7** were prepared by Gong using 4,4'-bipyridine and then substituting the respective RI group. [65] Ion exchange to the hexafluorophosphate salt afforded increased solubility of the paraquat salt in organic media. [45, 57]

To study supramolecular formation, ^{1}H NMR was used as the technique of choice and was performed by Gong. [63] Exchange is fast on the NMR time scale. [45, 57, 64] Thus, a series of titrations were performed on each system described below. In all cases, a specified mM concentration of host macrocycle in acetone was prepared in volumetric flasks. A small and exact amount of this solution was added to the NMR tube by volume; the remainder was used to prepare a known concentration of guest moieties. Titration was achieved by adding a defined volume of this paraquat guest and host macrocycle solution to the NMR tube. Thus, the initial component concentrations were known, while

the total host concentration remained constant. As expected, once individual hosts and guests were mixed, charge transfer yielded an immediate orange solution. This indicates the rapid formation of a [2]pseudorotaxane via through-space π-stacking interactions of host and guest.[45, 57]

Employing respective iterative graphical methods described above, association constants, and in two cases thermodynamic data, have been determined. In every instance, errors have been determined using a confidence interval about the mean at the 95% level according to Equation 23 for plots in the form y = mx + b

$$\Delta K_a = K_a \sqrt{\left(\frac{\Delta b}{b}\right)^2 + \left(\frac{\Delta m}{m}\right)^2} \tag{23}$$

II.2.1.2 COMPLEXATION OF BIS(5-ACETOXY-1,3-PHENYLENE)-32-CROWN-10 WITH *N,N'*-BIS(*β*-HYROXYETHYL)-4,4'-BISPYRIDINIUM BIS(HEXA-FLUOROPHOSPHATE)

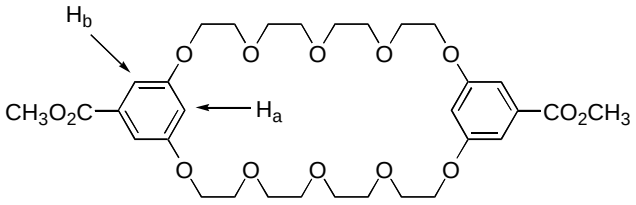

2

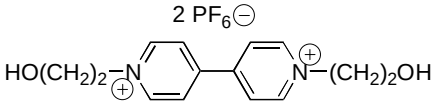

3

The binding of diester BMP32C10 (**2**) with paraquat diol **3** has been described utilizing the Benesi-Hildebrand graphical method. [63] Table 2 lists the chemical shifts of protons H_a and H_b of **2** upon complexation with specified concentrations of **3** at various temperatures. Here, the total concentration of **2** is kept constant at 7.584 mM. The time averaged signals of the pseudorotaxane complex are shifted upfield relative to

the uncomplexed state. Furthermore, increasing the temperature results in decreased relative Δ values ($\delta_{uncomplexed}$-$\delta_{observed}$), indicating an exothermic complexation process. [57]

^{1}H NMR data were interpreted using iterative Benesi-Hildebrand, Cresswell-Allred, and Rose-Drago Graphical Methods, which were then compared to previous non-iterative Benesi-Hildebrand values (Table 3). The calculated iterative values agree with each other, while the non-iterative Benesi-Hildebrand results underestimate the association constant. Gong et al. have pointed out that this underestimation results from the approximation that $[G]_0$ is used to estimate [G] in the first Benesi-Hildebrand iteration; the disparity is greater with increasing K_a values. [57]

Table 2. Chemical Shifts (400 MHz, acetone d-$_6$) of Protons H_a and H_b of **2** Upon Complexation with Various Amounts of **3** at Specified Temperatures.[a]

[3]$_0$ (mM)	**21.4 °C** δ_a/δ_b[b] (ppm)	**30.0 °C** δ_a/δ_b (ppm)	**38.0 °C** δ_a/δ_b (ppm)	**46.0 °C** δ_a/δ_b (ppm)	**54.0 °C** δ_a/δ_b (ppm)
0.00	6.724 / 7.092	6.729 / 7.098	6.736 / 7.106	6.741 / 7.114	6.746 / 7.117
12.60	6.546 / 6.948	6.589 / 6.990	6.625 / 7.025	6.656 / 7.052	6.681 / 7.074
17.65	6.507 / 6.915	6.555 / 6.965	6.597 / 7.005	6.632 / 7.035	6.661 / 7.061
26.36	6.461 / 6.878	6.514 / 6.933	6.560 / 6.977	6.601 / 7.014	6.637 / 7.045
42.51	6.402 / 6.831	6.457 / 6.889	6.507 / 6.939	6.554 / 6.981	6.596 / 7.017
53.52	6.374 / 6.808	6.427 / 6.865	6.477 / 6.913	6.525 / 6.961	6.572 / 7.001
81.67	6.330 / 6.771	6.371 / 6.826	6.427 / 6.879	6.473 / 6.924	6.526 / 6.968

[a] $[\mathbf{2}]_0$ held constant at 7.584 mM; temp ± 0.1 °C

[b] δ_a/δ_b: chemical shifts of protons H_a and H_b, respectively, ± 0.001 ppm.

Table 3. Association Constants as Determined for the Complexation of **2** with **3**.

			Benesi-Hildebrand[b]			Creswell-Allred[b]				Rose-Drago[b]		
Obs. Proton	**Temp** (^{o}C)	**K_a**[a] (M^{-1})	**K_a** (M^{-1})	**Δ_0**	**r^2**	**K_a** (M^{-1})	**Δ_0**	**r^2**	**$\delta_{int}/\delta_{free}$**[c]	**K_a** (M^{-1})	**Std. Dev.**	**Median**
H_a	*21.4*	44.1	64 ± 3	0.462	0.997	59 ± 3	0.475	0.997	0.99996	58 ± 5	10.4	57.5
H_b		43.7	63 ± 3	0.377	0.997	59 ± 3	0.387	0.996	0.99990	56 ± 5	9.2	55.7
H_a	*30.0*	33.1	45 ± 2	0.439	0.996	40 ± 2	0.464	0.994	0.99988	41 ± 5	10.2	39.3
H_b		33.6	46 ± 2	0.334	0.995	41 ± 2	0.353	0.995	0.99987	41 ± 5	10.7	40.2
H_a	*38.0*	26.8	35 ± 1	0.406	0.997	31 ± 1	0.432	0.997	0.99990	32 ± 4	8.4	31.3
H_b		27.6	34 ± 1	0.302	0.996	30 ± 1	0.323	0.996	0.99990	31 ± 5	9.1	30.0
H_a	*46.0*	20.7	26 ± 1	0.381	0.997	22 ± 1	0.418	0.996	0.99998	24 ± 4	6.8	23.4
H_b		22.5	29 ± 1	0.259	0.996	24 ± 1	0.286	0.994	0.99992	26 ± 5	9.0	23.9
H_a	*54.0*	17.6	22 ± 1	0.334	0.997	19 ± 1	0.336	0.996	0.99971	20 ± 3	6.4	18.4
H_b		16.9	21 ± 1	0.228	0.997	17 ± 1	0.257	0.996	0.99992	19 ± 3	6.7	17.3

[a] As determined by Gong et al. using the non-iterative Benesi-Hildebrand method [63], estimated relative error ± 5%

[b] Iterative methods

[c] The number of digits displayed does not suggest degree of significance. Rather, they are meant to illustrate the degree of convergence used to obtain K.

Van't Hoff plots confirm the exothermic formation of the above pseudorotaxane (Table 4, Figure 12). Not surprisingly, ΔS is negative as a result of supramolecular organization. ΔH is also negative, a consequence of strong supramolecular forces such as π-stacking, dipolar-dipolar interactions, and H-bonding between host and guest molecules.

Table 4. Changes in Enthalpy and Entropy as Determined via van't Hoff Plots for the Complexation of **2** with **3** in Acetone, Utilizing Graphical Methods.

Technique, Proton	**Slope** (K)	**Intercept**	**R^2**	**ΔH** (kJ mol^{-1})	**ΔS** (J $mol^{-1}K^{-1}$)
Benesi-Hildebrand[a]					
H_a	2743	-5.536	0.997	*-22.8*	*-46.0*
H_b	2727	-5.468	0.993	*-22.7*	*-45.5*
Benesi-Hildebrand[b]					
H_a	3195	-6.715	0.995	*-26.6 ± 0.1*	*-55.8 ± 0.0*
H_b	3157	-6.584	0.993	*-26.2 ± 0.2*	*-54.7 ± 0.0*
Creswell-Allred[b]					
H_a	3411	-7.537	0.990	*-28.4 ± 0.0*	*-62.7 ± 0.3*
H_b	3591	-8.121	0.996	*-29.9 ± 0.1*	*-67.5 ± 2.4*
Rose-Drago[b]					
H_a	3171	-6.728	0.996	*-26.4 ± 1.6*	*-55.9 ± 5.9*
H_b	3107	-6.530	0.994	*-25.8 ± 1.8*	*-54.3 ± 7.1*

[a] As determined by Gong et al. using the non-iterative method [63]

[b] Iterative methods

Importantly, the complex formation between **2** and **3** at room temperature is much weaker than the simple BMP32C10•Dimethyl Paraquat(PF_6^-)$_2$ complex reported by Stoddart et al. in 1987: 60 M^{-1} versus 760 M^{-1}. [45] As described by Gibson and others, solvent effects play a major role in pseudorotaxane formation. [65] Presumably, solvation of **3** is much greater than Stoddart's dimethyl paraquat due to **3**'s protic nature, thereby limiting host-guest interactions. Furthermore, the electron withdrawing ester group of the functionalized macrocycle undoubtedly detracts from neighboring host-guest π–π interaction relative to the unsubstituted macrocycle.

Figure 12. Representative van't Hoff Plot for the Complexation of **2** with **3**. Creswell-Allred Data Derived from H_a of **2** has Been Utilized.

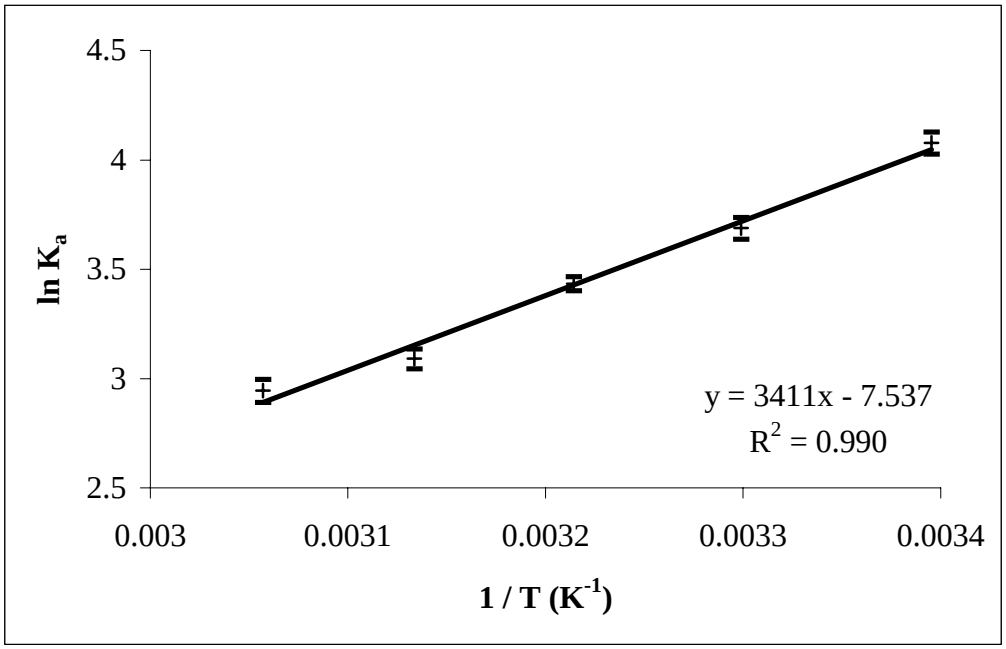

II.2.1.3 COMPLEXATION OF HYDROXYMETHYL BMP32C10 WITH PARAQUAT DIACID

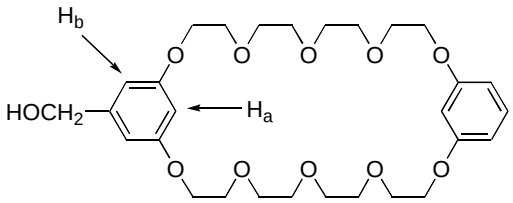

4

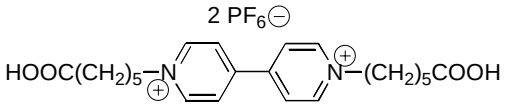

5

As above, the binding of hydroxymethyl BMP32C10 **4** with paraquat diacid **5** has been described utilizing the Benesi-Hildebrand graphical method. [63] Table 5 lists the chemical shifts of protons H_a and H_b of **4** upon complexation with specified concentrations of **5** at various temperatures. Here, the total concentration of **5** is kept constant at 6.889 mM.

Table 6 describes binding based on the three models[†]. Given its degree of uncertainty and relatively large association constants, the Rose-Drago model seems to do an especially poor job at describing the complex formed between **4** and **5**. Herein lies the basis of the argument discussed above over which method to use: it is difficult to predict in what instance which method will fail and which will prevail. Again, working with as many models as possible will allow the discerning chemist to draw a general conclusion consistent with his/her results.

ΔH and ΔS values (Table 7) are generally larger in magnitude than the complex formed between **2** and **3** (Table 4), most likely an indicator of the greater degree of hydrogen bonding between **4** and **5** relative to **2** and **3**.

[†] The importance of using iterative techniques to determine association constants can also be readily noted from table 6, where the association described by the non-iterative Benesi-Hildebrand technique is underestimated by 400 to 500 percent relative to the iterative techniques!

Table 5. Chemical Shifts (400 MHz, acetone-d_6) of Protons H_a and H_b of **4** Upon Complexation with Various Amounts of **5** at Specified Temperatures.[a]

$[5]_0$ (mM)	21.4 °C δ_a/δ_b[b] (ppm)	30.0 °C δ_a/δ_b (ppm)	38.0 °C δ_a/δ_b (ppm)	46.0 °C δ_a/δ_b (ppm)	54.0 °C δ_a/δ_b (ppm)
0.00	9.492 / 8.867	9.484 / 8.860	9.476 / 8.851	9.469 / 8.844	9.462 / 8.836
3.51	9.406 / 8.687	9.413 / 8.709	9.419 / 8.730	9.423 / 8.747	9.426 / 8.761
6.92	9.353 / 8.571	9.369 / 8.611	9.383 / 8.648	9.394 / 8.681	9.402 / 8.708
10.43	9.317 / 8.494	9.337 / 8.541	9.356 / 8.586	9.371 / 8.627	9.383 / 8.664
13.9	9.295 / 8.448	9.315 / 8.493	9.335 / 8.539	9.352 / 8.585	9.367 / 8.627
17.47	9.283 / 8.420	9.301 / 8.461	9.320 / 8.506	9.339 / 8.554	9.355 / 8.598
20.68	9.273 / 8.400	9.290 / 8.433	9.308 / 8.479	9.327 / 8.527	9.343 / 8.572
27.42	9.261 / 8.375	9.275 / 8.405	9.292 / 8.444	9.310 / 8.489	9.326 / 8.535

[a] $[\mathbf{4}]_0$ held constant at 6.889 mM; temp ± 0.1 °C

[b] δ_a/δ_b: chemical shifts of protons H_a and H_b, respectively, ± 0.001 ppm.

Table 6. Association Constants as Determined for the Complexation of **4** with **5**.

			Benesi-Hildebrand[b]			*Creswell-Allred*[b]				*Rose-Drago*[b]		
Obs. Proton	**Temp** (^oC)	K_a[a] (M^{-1})	K_a (M^{-1})	Δ_0	r^2	K_a (M^{-1})	Δ_0	r^2	$\delta_{int}/\delta_{free}$[c]	K_a (M^{-1})	**Std. Dev.**	**Median**
H_a	*21.4*	102.0	494 ± 58	0.244	0.996	398 ± 19	0.256	0.999	0.999990	328 ± 43	99.0	300.1
H_b		97.2	413 ± 47	0.538	0.999	369 ± 10	0.552	1.000	0.999983	333 ± 59	59.1	307.1
H_a	*30.0*	87.2	323 ± 36	0.229	0.995	254 ± 11	0.244	0.999	0.999998	214 ± 64	64.3	191.0
H_b		82.2	268 ± 28	0.52	0.998	230 ± 6	0.544	0.999	0.999983	214 ± 49	48.6	201.9
H_a	*38.0*	73.8	221 ± 22	0.211	0.995	167 ± 7	0.231	0.998	0.999988	145 ± 22	50.7	126.1
H_b		65.7	168 ± 16	0.504	0.999	148 ± 3	0.523	1.000	0.999970	141 ± 11	26.0	133.7
H_a	*46.0*	66.0	176 ± 17	0.187	0.994	125 ± 5	0.212	0.997	0.999988	117 ± 21	47.0	99.8
H_b		56.4	127 ± 11	0.463	0.998	104 ± 2	0.500	0.999	0.999992	103 ± 10	21.9	95.9
H_a	*54.0*	56.0	127 ± 11	0.171	0.996	88 ± 4	0.198	0.997	0.999996	85 ± 14	31.5	77.8
H_b		46.8	91 ± 7	0.429	0.999	74 ± 2	0.474	0.999	0.999966	73 ± 8	18.2	67.8

[a] As determined by Gong et al. using the non-iterative Benesi-Hildebrand method [63], estimated relative error ± 5%

[b] Iterative methods

[c] The number of digits displayed does not suggest degree of significance. Rather, they are meant to illustrate the degree of convergence used to obtain K.

Table 7. Changes in Enthalpy and Entropy as Determined via van't Hoff Plots for the Complexation of **4** with **5** in Acetone, Utilizing Respective Graphical Methods.

Technique, Proton	Slope (K)	Intercept	R^2	ΔH (kJ mol^{-1})	ΔS (J $mol^{-1}K^{-1}$)
Benesi-Hildebrand [a]					
H_a	2743	-5.536	0.997	*-22.8*	*-46.0*
H_b	2727	-5.468	0.993	*-22.7*	*-45.5*
Benesi-Hildebrand [b]					
H_a	3955	-7.257	0.995	*-32.9 ± 0.7*	*-60.3 ± 1.4*
H_b	4504	-9.283	0.996	*-37.4 ± 0.9*	*-77.2 ± 2.0*
Creswell-Allred [b]					
H_a	2529	-3.453	0.998	*-36.8 ± 0.1*	*-75.5 ± 0.1*
H_b	2665	-4.279	0.999	*-39.6 ± 0.1*	*-85.5 ± 0.0*
Rose-Drago [b]					
H_a	3934	-7.599	0.993	*-32.7 ± 1.7*	*-63.2 ± 7.9*
H_b	4477	-9.406	0.999	*-37.2 ± 1.1*	*-78.2 ± 5.1*

[a] As determined by Gong et al. using the non-iterative method [63]

[b] Iterative methods

II.2.1.4 COMPLEXATION OF DIACID BMP32C10 WITH PARAQUAT DIOL

Three iterative graphical methods (Benesi-Hildebrand, Rose-Drago, and Cresswell-Allred) were engaged to determine the association constant for the pseudorotaxanes formed upon complexation of BMP32C10 diacid (**6**) with paraquat diol **3** and upon complexation of hydroxymethyl BMP32C10 (**4**) with paraquat diester **7**. The complexation of **6** + **3** has previously been studied utilizing the non-iterative Benesi-Hildebrand graphical method. [63] ^{1}H NMR data was collected at 21.4 ± 0.1 ^{o}C. $[\mathbf{6}]_0$ was held constant at 8.484 mM and titrated systematically with **3**. Tables 8 and 9 list the results.

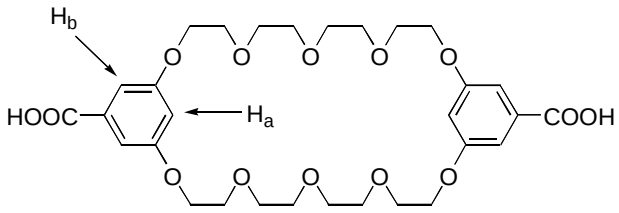

6

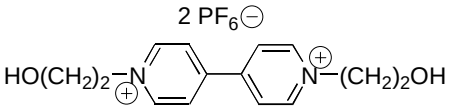

3

Table 8. Chemical Shifts (400 MHz, 21.4 °C, acetone-d_6) of Protons H_a and H_b of **6** Upon Complexation with Various Amounts of **3**.[a]

sample	$[3]_0$ (mM)	δ_a (ppm)	δ_b (ppm)
1	0.00	6.757	7.152
2	14.64	6.520	6.967
3	28.54	6.428	6.895
4	47.11	6.370	6.846
5	58.28	6.344	6.829
6	71.70	6.325	6.811
7	94.95	6.297	6.792
8	121.40	6.279	6.777

[a] $[\mathbf{6}]_0$ held constant at 8.484 mM; temp ± 0.1 °C

Table 9. Association Constants as Determined for the Complexation of **6** with **3**.

			Benesi-Hildebrand [b]			***Creswell-Allred*** [b]				***Rose-Drago*** [b]		
Obs. Proton	**Temp** (°C)	K_a [a] (M^{-1})	K_a (M^{-1})	Δ_0	r^2	K_a (M^{-1})	Δ_0	r^2	$\delta_{int}/\delta_{free}$ [c]	K_a (M^{-1})	**Std. Dev.**	**Median**
H_a	*21.4*	51.5	77 ± 4	0.521	0.997	74 ± 4	0.530	0.996	0.9997	64 ± 4	9.4	64.8
H_b		50.6	75 ± 4	0.410	0.998	72 ± 3	0.417	0.997	0.9998	63 ± 3	6.9	63.0

[a] As determined by Gong et al. using the non-iterative Benesi-Hildebrand method [63], estimated relative error ± 5%

[b] Iterative methods

[c] The number of digits displayed does not suggest degree of significance. Rather, they are meant to illustrate the degree of convergence used to obtain K.

II.2.1.5 COMPLEXATION OF HYDROXYMETHYL BMP32C10 WITH PARAQUAT DIESTER

Three iterative graphical methods (Benesi-Hildebrand, Rose-Drago, and Cresswell-Allred) were engaged to determine the association constant for the pseudorotaxanes formed upon complexation of hydroxymethyl BMP32C10 (**4**) with paraquat diester **7**. ^{1}H NMR data was collected at 21.4 ± 0.1 ^{o}C. $[\mathbf{4}]_0$ was held constant at 5.190 mM and titrated systematically with **7**. Tables 10 and 11 describe the results.

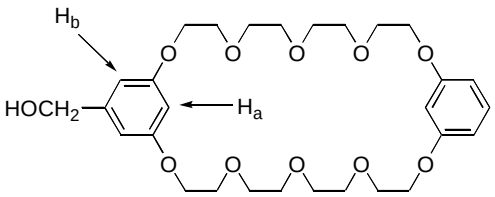

4

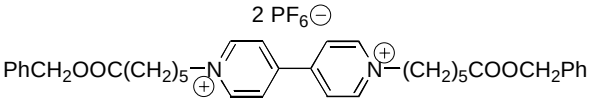

7

Table 10. Chemical Shifts (400 MHz, 21.4 ^{o}C, acetone-d_6)of Protons H_a and H_b of **4** Upon Complexation with Various Amounts of **7** in Acetone at 21.4 ^{o}C.[a]

sample	$[7]_0$ (mM)	δ_a (ppm)	δ_b (ppm)
1	0.0	9.470	8.849
2	2.1	9.410	8.720
3	3.8	9.370	8.632
4	10.3	9.294	8.465
5	13.4	9.278	8.433
6	17.7	9.263	8.400
7	21.5	9.257	8.385
8	28.1	9.246	8.362
9	42.5	9.233	8.340

[a] $[\mathbf{4}]_0$ held constant at 5.190 mM; temp ± 0.1 ^{o}C

Table 11. Association Constants as Determined for the Complexation of **4** with **7**.

		Benesi-Hildebrand [a]			***Creswell-Allred*** [a]				***Rose-Drago*** [a]		
Obs. Proton	**Temp (^{o}C)**	**K_a (M^{-1})**	**Δ_0**	**r^2**	**K_a (M^{-1})**	**Δ_0**	**r^2**	**$\delta_{int}/\delta_{free}$** [b]	**K_a (M^{-1})**	**Std. Dev.**	**Median**
H_a	*21.4*	375 ± 40	0.249	0.999	386 ± 39	0.249	0.999	0.999995	328 ± 14	36.6	336.3
H_b		357 ± 38	0.547	0.999	379 ± 18	0.540	0.999	0.999996	362 ± 40	107.2	347.5

[a] Iterative methods

[b] The number of digits displayed does not suggest degree of significance. Rather, they are meant to illustrate the degree of convergence used to obtain K.

II.2.1.6 COMPARISON OF FOUR SUPRAMOLECULAR COMPLEXES

Comparing the four common data sets at 21.4 ^{o}C, a few interesting observations are noted. First, the steric and/or electronic influence of **7**'s benzyl group appears to have little to no effect on its association with **4**. This conclusion is drawn based on the strength of association between **4** and **7** (iterative Benesi-Hildebrand, H_a: 375 ± 40, Creswell-Allred, H_a: 386 ± 38, Rose-Drago, H_a: 328 ± 14) compared to **4** and **5** (iterative Benesi-Hildebrand, H_a: 494 ± 58, Creswell-Allred, H_a: 398 ± 19, Rose-Drago, H_a: 328 ± 99), which substitutes a hydrogen for the benzyl. Prior to this comparison, there were generally two schools of thought about such complexation. A) If long enough, the flexible methylene spacers of **7** might permit the terminus to drive increased through-space interactions in the form of π-π interactions between guest benzyl and host phenyl. B) The bulkiness of **7** relative to **5** might hinder pseudorotaxane formation.

Secondly, the above results hint at substituent influences on complexation. Macrocycle **4** bears a single electron-donating group; macrocycles **2** and **6** bear two electron-withdrawing groups. As is expected due to the influence of π-π host-guest interactions, association is greatest for complexes involving host **4**: the magnitude of association between **6** and **3** (K_a = 74 M^{-1}, Creswell-Allred) is much less than that between **4** and **5** (K_a = 369 M^{-1}, Creswell-Allred), as well as between **4** and **7** (K_a = 386 M^{-1}, Creswell-Allred). These results agree well with the findings of Stoddart and co-workers, where they have noticed a linear free energy relationship between K_a and the Hammett substituent constants in similar pseudorotaxane formations. [66]

II.2.2 HIGHLY EFFICIENT GUEST BINDING: COMPLEXATION OF A 32-MEMBERED CRYPTAND WITH DIMETHYL PARAQUAT $(PF_6)_2$

II.2.2.1 INTRODUCTION

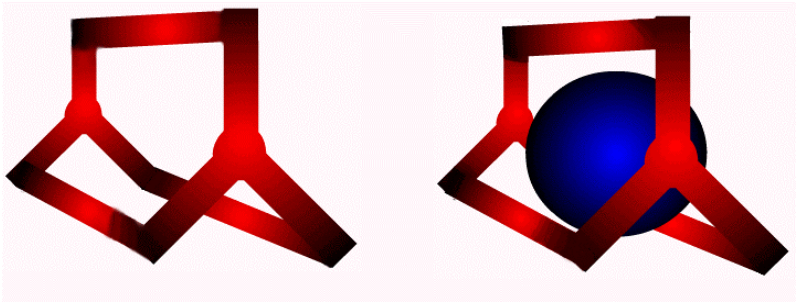

The use of cryptands, or bicyclic macrocycles **8**, as host receptors in pseudorotaxane-like formations **9** has been briefly discussed in Section II.1.2.1. Described by Dietrich and others, association constants of such preorganized structures as cryptands can be 10^3-10^4 times higher than those found in analogous unstrained macrocycles. [67] Fischer first implied this idea of preorganization in discussing the "lock and key" mechanism. [68] Others went on to show that simple macrocyclic hosts have a greater affinity for complexation than do their linear host counterparts, leading to the idea of a macrocyclic (a.k.a. preorganized) affect. [35] For a descriptive analysis on the concept of preorganization, the reader is referred to a review by Inoue and Wada. [69]

Also described in Section II.1.2.1 was the discovery of "cradled barbell" type supramolecular formations. Believing that the strength of association in the "exo" complex would be enhanced by closure of the folded macrocycle, a bicyclic crown ether was prepared and its complexation with an appropriate guest investigated. As discussed below, an increase of two orders in magnitude greater than the "exo" complex was found to exist in the cryptand pseudorotaxane-like inclusion formation. [70] Thus, chemists are moving towards the binding efficiency found in natural systems.

II.2.2.2 RESULTS

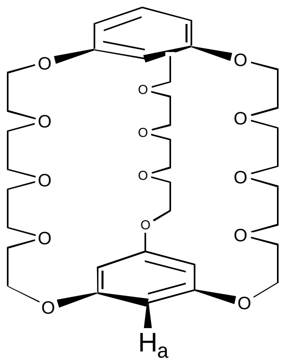

10

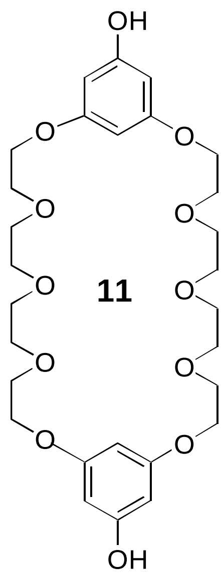

11

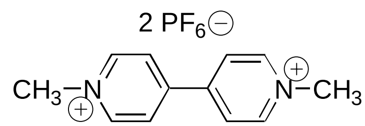

3

*II.2.2.2.1 Preparation of Bis(1,3,5-phenylene)tri(1,4,7,10,13-pentaoxytridecyl) (**10**). [70]*

Bis(1,3,5-phenylene)tri(1,4,7,10,13-pentaoxytridecyl) (**10**) was prepared in one step from bisphenol **11** and tetra(ethylene glycol) ditosylate using the high dilution technique. [64, 70] ^{1}H NMR ($CDCl_3$) δ 6.00 (s, 6H, ArH), 3.93 (t, 12H, α-OCH_2), 3.81 (t, 12H, β-OCH_2), 3.69 (m, 12H, γ-, δ-OCH2). ^{13}C NMR ($CDCl_3$) δ 160.41, 94.20, 70.94, 70.64, 69.66, 67.47. Mass Spectrum (High-resolution FABMS (3-NBA)) m/z $(M + Na)^+$ 749.3373.

*II.2.2.2.2 Complexation Studies with **10**.*

0.75 mL of a 0.100 mM solution of **10** (3.63 x 10^{-4} g, or 4.98 x 10^{-7} mol, in a 5 mL volumetric flask) in acetone-d_6 was carefully transferred to a dry NMR tube via a high precision syringe, and the tube capped and sealed with parafilm prior to recording ^{1}H NMR spectra at various temperatures. To this, incremental and specific volumes of a stock paraquat **3** solution (see below) were added, the tube resealed, and spectra observed at all temperatures. (Table 12, Figure 13). A vivid, persistent yellow color ensued upon addition of paraquat to the cryptand solution, indicative of a charge-transfer inclusion complex. NMR data afforded measurements of association constants at each temperature

Table 12. Chemical Shifts (400 MHz, acetone-d_6) of Proton H_a **10** Upon Complexation with Various Amounts of **3** at Specified Temperatures.[a]

$[\mathbf{3}]_0$ (mM)	30.0 ^{o}C δ_a (ppm)	38.0 ^{o}C δ_a (ppm)	46.0 ^{o}C δ_a (ppm)	54.0 ^{o}C δ_a (ppm)
0.000	5.812	5.826	5.840	5.855
0.039	5.684	5.719	5.753	5.788
0.078	5.621	5.661	5.707	5.750
0.117	5.545	5.598	5.649	5.698
0.156	5.495	5.541	5.591	5.644
0.195	5.478	5.521	5.569	5.621
0.272	5.453	5.489	5.532	5.582
0.387	5.436	5.467	5.506	5.553

[a] $[\mathbf{10}]_0$ held constant at 0.100 mM; temp ± 0.1 ^{o}C

[b] δ_a: chemical shift of protons H_a, ± 0.001 ppm.

Figure 13. ^{1}H NMR Spectra (400 MHz, acetone-d_6, 30.0 ^{o}C) of cryptand **10** (a, top spectrum), paraquat **3** (d, bottom), a solution of 0.100 mM **10** + 0.039 mM **3** (b, second from top), and a solution of 0.100 mM **10** + 0.117 mM **3** (c, second from bottom).

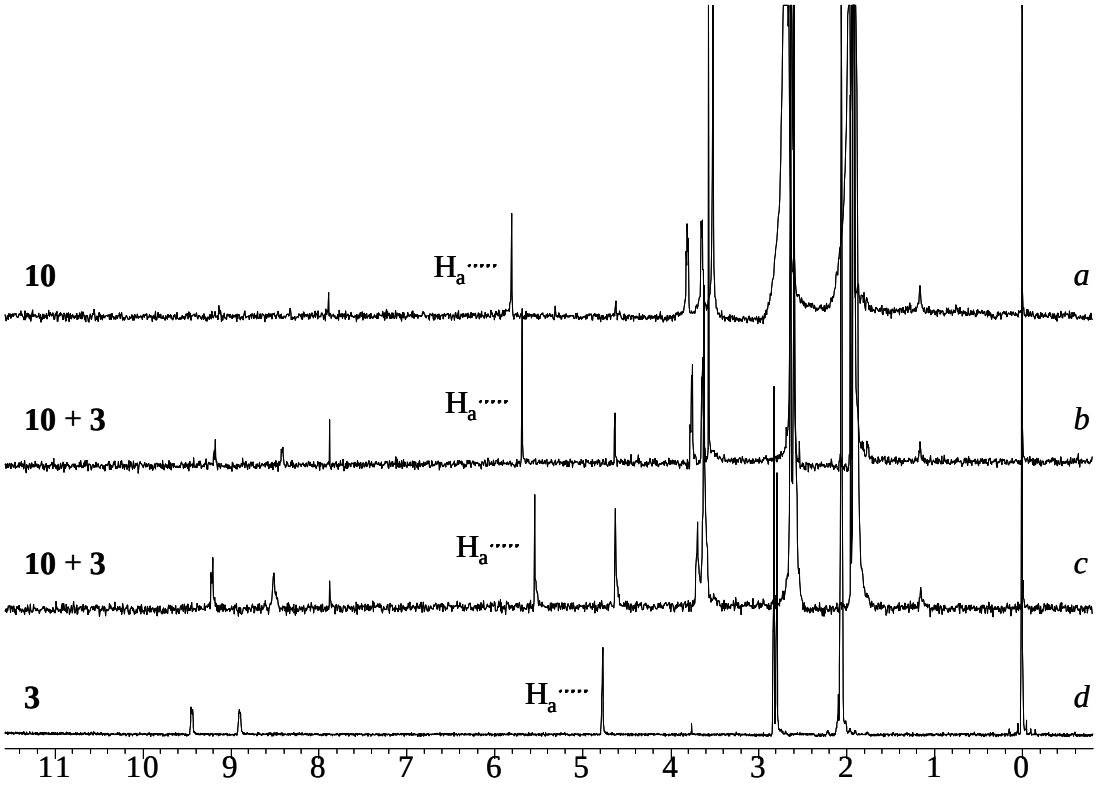

Table 13. Association Constants as Determined for the Complexation of **10** with **3**.

		Creswell-Allred [a]				*Rose-Drago* [a]		
Obs. Proton	**Temp** (^{o}C)	K_a (M^{-1})	Δ_0	r^2	$\delta_{int}/\delta_{free}$ [b]	K_a (M^{-1})	**Std. Dev.**	**Median**
H_a	*30.0*	$4.10 \pm 0.70 \times 10^4$	0.408	0.990	0.99999985	$4.21 \pm 2.64 \times 10^4$	6.17×10^4	2.71×10^4
H_a	*38.0*	$2.01 \pm 0.21 \times 10^4$	0.424	0.992	0.99999972	$1.47 \pm 0.69 \times 10^4$	1.62×10^4	1.56×10^4
H_a	*46.0*	$1.08 \pm 0.11 \times 10^4$	0.444	0.989	0.99999937	$1.07 \pm 0.27 \times 10^4$	5.76×10^3	1.27×10^4
H_a	*54.0*	$6.44 \pm 0.58 \times 10^3$	0.467	0.987	0.99999992	$6.36 \pm 2.09 \times 10^3$	4.52×10^3	6.40×10^3

[a] Iterative methods

[b] The number of digits displayed does not suggest degree of significance. Rather, they are meant to illustrate the degree of convergence used to obtain K.

studied via the iterative Cresswell-Allred and Rose-Drago techniques (Table 13). The data were also analyzed using the iterative Benesi-Hildebrand program. However, perhaps due to the uneven weighing of data points in such a strongly binding system (only the first four data points fall within the 20 to 80% binding regime, the last three points extend beyond 80% loading), (see Appendix I, Figure 1), [71] the iterative slope switches from positive to negative, thereby resulting in a failed analysis. In addition, van't Hoff plots yielded the thermodynamic parameters ΔH and ΔS (Table 14). Errors are determined as described in section II.2.1.1.

II.2.2.2.3 Preparation of Stock Paraquat Solution

0.279 g of **3** (5.87×10^{-4} mol) was transferred into a 10 mL volumetric flask and diluted with acetone to yield a 5.87×10^{-2} M solution, 1 mL of which was subsequently transferred to a 2 mL volumetric flask prior to solvent removal via a vacuum oven. The residual 2.79×10^{-2} g of **3** was then taken up in 2 mL of the 9.95×10^{-5} M solution of **10** described above to yield a stock solution consisting of 9.95×10^{-5} M **10** and 2.94×10^{-2} M **3**. Specified volumes of this stock solution were used to titrate a known volume of **10** inside a NMR tube. In this manner, the concentration of **10** remains constant while **3** continuously loads into the system.

Table 14. Changes in Enthalpy and Entropy as Determined via van't Hoff Plots for the Complexation of **10** with **3** in Acetone.

Technique	**Slope** (K)	**Intercept**	**R^2**	**ΔH** (kJ mol^{-1})	**ΔS** (J $mol^{-1}K^{-1}$)
Creswell-Allred	7662	-14.688	0.998	*-63.7 ± 17.2*	*-122 ± 6*
Rose-Drago	9718	-32.170	0.920	*-57.9 ± 11.7*	*-104 ± 35*

II.2.2.3 DISCUSSION

Gibson et al. have shown the association constant between bisphenol **11** and **3** to be 5.7 x 10^2 M^{-1} at ambient temperatures, corresponding to a change in free energy of -21 kJ mol^{-1}. [70] Stoddart and co-workers have demonstrated the association constant between unsubstituted BMP32C10 and **3** to be 5.6 x 10^2 M^{-1}, with a change in free energy of -16 kJ mol^{-1}. [45] Under slightly less favorable reaction conditions, i.e., association decreases with increasing temperature in exothermic reactions, the association between **10** and **3** at 30.0 ^oC is shown to be 4.10 x 10^4 M^{-1} using the iterative Cresswell-Allred method. This corresponds to a change in free energy of -27 kJ mol^{-1}. At 23 ^oC, the association between **10** and **3** at has been shown to be 6.1 x 10^4 M^{-1}, corresponding to a change in free energy of -28 kJ mol^{-1}. [70] Earlier work has demonstrated through the construction of Job plots that binding occurs in 1:1 stoichiometry; FABMS and X-ray diffraction results confirm the 1:1 complex. [70]

II.2.2.4 CONCLUSION

As expected, the binding of paraquat **3** by the strained bicyclic system **10** is much stronger than the binding found in analogous unstrained macrocycles. Increasing binding strength will allow the chemist to design much more robust supramolecular assemblies than have been previously demonstrated. Whereas much of the current interest in supramolecular polymers involves quadruple hydrogen bond arrays, [52] the strength of association in preorganized host systems such as bicyclic **10** will surely push supramolecular polymeric assembly to the next level.

II.3.0 REFERENCES

[1] Cowie, J. M. G. *Polymers: Chemistry and Physics of Modern Materials*. Intertext Books: London, **1973**, a.) 263. b.) 271.

[2] Gibson, H. W.; Bheda, M. C.; Engen, P. T. *Prog. Polym. Sci.* **1994**, *19*, 844.

[3] Roover, J.; Toporowski, P. M. *J. Polym. Sci., Polym. Phys*. **1988**, *26*, 125.

[4] Semylen, J. A., ed. *Cyclic Polymers*. Elsevier Applied Science: New York, **1986**.

[5] Odian, G. *Principles of Polymerization*. John Wiley & Sons: New York, **1981**, 2nd Ed., a.) 18, b.) 401, c.) 113.

[6] Riess, G.; Hurtrez, G.; Bahadur, P. *Encyl. Polym. Sci. Eng.* Wiley: New York, **1985**, 2nd Ed., 324-434.

[7] Noshay, A.; McGrath, J. E. *Block Copolymers: Overview and Critical Survey*. Academic Press, Inc.: New York, **1977**.

[8] a) Newkome, G. R., ed. *Advances in Dendritic Macromolecules*. JAI Press Inc.: Stamford, **1999**, vol. 4. b) Newkome, G. R.; Moorefield, C. N.; Vögtle, F.; Eds. *Dendritic Molecules: Concepts, Syntheses, Perspectives***.** Wiley-VCH: Weinheim, **1996**.

[9] Meijer, D. J., ed. *Block Copolymers: Science and Technology*. MMI Symposium Series, Harwood Academic Publishers, **1983**.

[10] Allcock, H. R.; Lampe, F. W. Contemporary Polymer Chemistry. Prentice-Hall Inc.: New Jersey, **1990**, 2nd Ed., a.) 5, b.) 12.

[11] Elias, H. G. Macromolecules. Plenum Press: New York, **1984**, ch. 34.

[12] Frisch, H. L.; Wasserman, E. *J. Am. Chem. Soc.* **1961**, *83*, 3789.

[13] a.) Frisch, H. L.; Martin, Il; Mark, H. *Monatsh.* **1953**, *84*, 250. b.) Fatat, F.; Derst, P. *Angew. Chem.* **1959**, *71*, 105.

[14] Schill, G.; Zöllenkopf, H. *Nachr. Chem. Techn.* **1967**, *79*, 149.

[15] For reviews of catenanes, see a) p 848-852 of reference 2 and b) Raymo, F. M.; Stoddart, J. F. *Chem. Rev.* **1999**, *99*, 1643.

[16] Harrison, I. T.; Harrison, S. J. *J. Am .Chem. Soc.* **1967**, *89*, 5723.

[17] Harrison, I. T. *J. Chem. Soc. Chem. Comm*. **1972**, 231.

[18] Harrison, I. T. J. *Chem. Soc. Perk. Trans. 1* **1974**, 301.

[19] Schill, G.; Beckmann, W.; Schweickert, N.; Fritz, H. *Chem. Ber*. **1986**, *119*, 2647.

[20] For a discussion of the coining of "crown ethers", see reference 14.

[21] Pedersen, C. J. *J. Am. Chem. Soc.* **1967**, *89*, a.) 2495 b.) 7017.

[22] Ball, P. *Designing the Molecular World: Chemistry at the Frontier*. Princeton University Press: Princeton, **1994**, 159.

[23] Cram, D. J.; Cram, J. M. *Science* **1974**, *183*, 803.

[24] Pedersen, C. J.; Frensdorff, H. K. *Angew. Chem. Int. Ed. Engl*. **1972**, *11*, 16.

[25] Frensdorff, H. K. *J. Am. Chem. Soc.* **1971**, *93*, 4685.

[26] Goldberg, I. *Acta Crystallogr., Sect. B* **1975**, *31*, 2592.

[27] Agam, G.; Graiver, D.; Zilkha, A. *J. Am. Chem. Soc.* **1976**, *98*, 5206.

[28] Agam, G.; Zilkha, A. *J. Am. Chem. Soc.* **1976**, *98*, 5214.

[29] Timko, J. M.; Helgeson, R. C.; Newcomb, M.; Gokel, G. W.; Cram, D. J. *J. Am. Chem. Soc.* **1974**, *96*, 7097.

[30] Metcalf, J. C.; Stoddart, J. F.; Jones, G. *J. Am. Chem. Soc.* **1977**, *99*, 8317.

[31] Colquhoun, H. M.; Stoddart, J. F. *J. Chem. Soc., Chem. Commun.* **1981**, 612.

[32] Shen. Y. X.; Zie, D.; Gibson, H. W. *J. Am. Chem. Soc.* **1994**, *116*, 537.

[33] a) Gibson, H. W.; Liu, S.; Lecavalier, P.; Wu, C.; Shen, Y. X. *J. Am. Chem. Soc.* **1995**, *117*, 852. b) Gong, C.; Gibson, H. W. *J. Am. Chem. Soc.* **1997**, *119*, 8585-8591. c) Gong, C.; Gibson, H. W. *Angew. Chem. Int. Ed.* **1997**, *36*, 2331-2333. d) Gong, C.; Subramanian, C.; Ji Q.; Gibson, H. W. *Macromolecules* **1998**, *31*, 1814-1818.

[34] a) Gibson, H. W.; Marand. H.; Liu, S. *Adv. Mater.* **1993**, *5*, 11. b) Gibson, H. W.; Liu, S.; Gong, C.; Joseph, E. *Macromolecules* **1997**, *30*, 3711-3727. c) Gong; Gibson, H. W. *Angew. Chem. Int. Ed.* **1998**, *37*, 310-314.

[35] Gokel, G. W. *Crown Ethers and Cryptands*. The Royal Society of Chemistry: Cambridge, **1991**.

[36] Gokel, G. W.; Nakano, A. *Crown Compounds: Toward Future Applications*. Cooper, S. R.; Ed. VCH Publishers, Inc.: New York, NY, **1992**; Ch. 1, p. 5.

[37] Truter, M. R. *Structure and Bonding* **1973**, *16*, 71.

[38] a) Ashton, P. R.; Fyfe, M. C. T.; Martinez-Diaz, M. V.; Menzer, S.; Schiavo, C.; Stoddart, J. F.; White, A. J. P.; Williams, D. J. *Chem. Eur. J.* **1998**, *8*, 1523. b)

Bryant, W. S.; Guzei, I. A.; Rheingold, A. L.; Gibson, H. W. *Org. Lett.* **1999**, *1*, 47.

[39] Izatt, R. M.; Lamb, J. D.; Rossiter, B. E.; Christensen, J. L.; Haymore, B. L. *J. Am .Chem. Soc* **1979**, *101*, 6273.

[40] Lehn, J. -M.; Vierling, P. *Tetrahedron Lett*. **1980**, 1323.

[41] Gokel, G. W.; Abel, E. *Complexation of Organic Cations*. Gokel, G. W.; Abel, E.; Eds. Pergamon: Oxford, UK, **1997**; Vol. 1, 511.

[42] Bovill, M. J.; Chadwick, D. J.; Johnson, M. R.; Jones, N. F.; Sutherland, I. O.; Newton, R. F. *J. Chem. Soc., Chem. Commun.* **1979**, 1065.

[43] Bradshaw, J. S.; Izatt, R. M.; Bordunov, A. V.; Zhu, C. Y.; Hathaway, J. K. *Crown Ethers*. Bradshaw, J. S.; Izatt, R. M.; Bordunov, A. V.; Zhu, C. Y.; Hathaway, J. K.; Eds. Pergamon: Oxford, UK, **1997**, Vol. 1, 35.

[44] a) Johnson, M. R.; Sutherland, I. O.; Newton, R. F. *J. Chem. Soc., Perkin. Trans. 1* **1979**, 357. b) Leigh, S. J.; Sutherland, I. O. *J. Chem. Soc., Perkin. Trans. 1* **1979**, 1089. c) Hodgkinson, L. C.; Johnson, M. R.; Leigh, S. J.; Spencer, N.; Sutherland, I. O.; Newton, R. F. *J. Chem. Soc., Perkin. Trans. 1* **1979,** 2193, d) Pearson, D. P. J.; Leigh, S. J.; Sutherland, I. O. *J. Chem. Soc., Perkin. Trans. 1* **1979**, 3113. e) Chadwick, D. J.; Cliffe, I. A.; Newton, R. F.; Sutherland, I. O. *J. Chem. Soc., Perkin Trans. 1* **1984**, 1707. f) Johnson, M. R.; Jones, N. F.; Sutherland, I. O. *J. Chem. Soc., Perkin Trans. 1* **1985**, 1637.

[45] Allwood, B. L.; Shahriarizavareh, H. Stoddart, J. F.; Williams, D. J. *J. Chem. Soc., Chem. Commun.* **1987**, 1058.

[46] a) Kolchinski, A. G.; Busch, D. H.; Alcock, N. W. *J. Chem. Soc., Chem. Commun.* **1995**, 1289. b) Ashton, P. R.; Campbell, P. J.; Chrystal, E. J. T.; Glinke, P. T.; Menzer, S.; Philp, D.; Spencer, N.; Stoddart, J. F.; Tasker, P. A.; Williams, D. J. *Angew. Chem. Int. Ed.* **1995**, *34*, 1865.

[47] For a thorough review of the various complexes prepared prior to 1999, see Fyfe, M. C. T.; Stoddart, J. F. *Adv. Supramol. Chem.* **1999**, *5*, 1.

[48] Wang, W.; Wei, B.; Wang, Q. *J. Crystallogr. Spectrosc. Res.* **1990**, *20*, 79.

[49] a) Mammen, M.; Simanek, E. E.; Whitesides, G. M. *J. Am. Chem. Soc.* **1996**, *2*, 989. b) Mammen, M.; Shakhnovich, E. I.; Deutch, J. M.; Whitesides, G. M. *J.*

Org. Chem. **1998**, *63*, 3821. c) Marsh, A.; Silvestri, M.; Lehn, J. -M. *J. Chem. Soc., Chem. Commun.* **1996**, 1527. d) Lehn, J. -M. *Makromol. Chem., Macromol. Symp.* **1993**, *69*, 1.

[50] Watson, J. D.; Crick, F. H. C. *Nature* **1953**, *171*, 737.

[51] Ashton, P. R.; Fyfe, M. C. T.; Hickingbottom, S. K.; Menzer, S.; Stoddart J. F.; White, A. J. P.; Williams, D. J. *Chem. Eur. J.* **1998**, *4*, 577.

[52] a) Sartorius, J.; Schneider, H.-J. *Chem. Eur. J.* **1996**, *2*, 1446. b) Sijbesma, R. P.; Beijer, F. H.; Brunsveld, L.; Folmer, B. J.; Hirschberg, J. H.; Lange, R.; Lowe, J. K. L.; Meijer, E. W. *Science* **1997**, *278*, 1601. c) Hirschberg, J. H.; Brunsveld, L.; Ramzi, A.; Vekemans, J. A.; Sijbesma, R. P.; Meijer, E. W. *Nature* **2000**, *407*, 167.

[53] a) Yamaguchi, N.; Nagvekar, D.; Gibson, H. W. *Angew. Chem.* **1998**, 110, 2518; *Angew. Chem. Int. Ed.* **1998**, *37*, 2361. b) Yamaguchi, N.; Hamilton, L. M.; Gibson, H. W. *Angew. Chem.* **1998**, 110, 3463; *Angew. Chem. Int. Ed.* **1998**, *37*, 3275.

[54] Tsukube, H.; Furuta, H.; Odani, A.; Takeda, Y.; Kudo, Y.; Inoue, Y.; Liu, Y.; Sakamoto, H.; Kimura, K. *Compreshensive Supramolecular Chemistry*; Davies, J. E. D.; Ripmeester, J. A.; Eds. Pergamon: Oxford, UK, **1997**, Vol. 8, 425.

[55] Benesi, H.; Hildebrand, J. H. *J. Am. Chem. Soc.* **1949**, *71*, 2703.

[56] Increasing salt concentration in solution necessarily complicates data analysis. In cases where it is inappropriate to continually add host molecules into a system, usually due to an insufficient supply, the ionic potential influence is neglected.

[57] Gong, C.; Balanda, P. B.; Gibson, H. W. *Macromolecules* **1998**, *31*, 5278.

[58] Scatchard, *G. Ann. N.Y. Acad. Sci.* **1949**, *51*, 660.

[59] Rose, N. J.; Drago, R. S. *J. Am. Chem. Soc.* **1959**, *81*, 798.

[60] Wachter, H. N.; Fried, V. *J. Chem. Ed.* **1974**, *51*, 798.

[61] Cresswell, C. J.; Allred, M. L. *J. Phys. Chem.* **1962**, *66*, 1469.

[62] Conors, K. A. *Binding Constants: The Measurement of Molecular Complex Stability*. John Wiley & Sons: New York, NY, **1987**, 68.

[63] Gong, C. *Linear, Branched, and Crosslinked Polyesters, Polyurethanes, and Polymethacrylates Derived From Rotaxane Formation: Syntheses and Properties*. Ph. D. Dissertation, Virginia Polytechnic Institute and State University, **1997**.

[64] Gibson, H. W.; Nagvekar, D. S. *Can. J. Chem.* **1997**, *75*, 1375.

[65] Shen, Y. X.; Engen, P. T.; Berg, M. A. G.; Merola, J. S.; Gibson, H. W. *Macromolecules* **1992**, *25*, 2786.

[66] Ashton, P. R.; Fyfe, M. C. T.; Hickingbottom, S. K.; Stoddart, J. F.; White, A. J. P.; Williams, D. J. *J. Chem. Soc., Perkin Trans. 2* **1998**, 2117.

[67] a) Dietrich, B. In *Comprehensive Supramolecular Chemistry*. Atwood, J. L.; Davies, J. E. D.; MacNicol, D. D.; Vögtle, F.; Series Eds. Pergamon Press: New York, NY, **1996**, Vol. 1. Gokel, G. Vol. Ed., 153. b) Lehn, J.-M. *Supramolecular Chemistry*. VCH Publishers: New York, NY, **1995**.

[68] Fischer, E. *Chem. Ber*. **1894**, *27*, 2985.

[69] Inoue, Y.; Wada, T. *Adv. Supramol. Chem.* **1997**, *4*, 55.

[70] Bryant, W. S.; Jones, J. W.; Mason; P. E.; Guzei, I.; Rheingold, A. L.; Fronczek, F. R.; Nagvekar, D. S.; Gibson, H. W. *Org. Lett.* **1999**, *1*, 1001.

[71] Bruce, M. R. *J. Chem. Educ.* **1997**, *74*, 1238.